THE CHEMICAL COMPOSITION AND DISTRIBUTION OF INTERSTELLAR GRAINS

J. MAYO GREENBERG and SEUNG-SOO HONG

State University of New York at Albany and Dudley Observatory, Albany, N.Y., U.S.A.

Abstract. The chemical composition of interstellar grains is derived here on the basis of (1) the cosmic abundance of the elements; (2) the wavelength dependence of extinction and polarization; (3) the average total extinction; (4) the ratio of polarization to extinction; (5) the predominantly dielectric character of grains in the visible spectral region; and (6) infrared spectral characteristics of grains. It is indicated that the major portion of the grains, by mass, consist of core-mantle particles in the 0.1-μm size range, whose cores consist largely of silicates and whose mantles are a solid mixture of O, C, and N with H in a heterogeneous combination of simple and complex molecules with frozen free radicals. A minor constituent of the solid particles exist in the form of very small uncoated particles generally less than 10^{-6} cm in size whose precise composition is not certain. Inferences of the core-mantle model with respect to spatial distribution are consistent with the proposition that growth of the mantles occurs in the galactic shock region predicted by the density-wave theory. Estimates of the total visual extinction toward the galactic center and the consequent estimates of the total amount of far infrared radiation are shown to depend critically on the grain model. Variations of the ratio of far ultraviolet to visual extinction are correlated with the conditions for growth of mantles on the bare small particles which are generally prevented from accreting mantles primarily because of their extreme temperature fluctuations produced by the ultraviolet photons in the radiation field.

I. Introduction

Since the early establishment of the solid particle nature of interstellar grains, a wide variety of possible candidates for their material constituents have been proposed. Initially, iron particles (Schalen, 1936; Greenstein, 1938) were considered largely because of the then current belief that meteorites were of cosmic origin. In a very significant way the circle is being closed and nowadays this basic concept is a most serious consideration as will be discussed later. Subsequently the suggestion by B. Lindblad (1935) that the grains could condense (or more properly, accrete) directly out of the interstellar medium led to the likelihood that ices of water, methane, and ammonia would be the major grain constituents (van de Hulst, 1943). This hypothesis appeared to be supported by the correlation between gas concentration and extinction. In the meanwhile the discovery of interstellar polarization by Hall (1949) and Hiltner (1949) led to some apparent difficulties in accounting for the observed amount of polarization relative to extinction. Even ideal alignment mechanisms seemed to preclude the ices (van de Hulst, 1957). Cayrel and Schatzman (1954) attempted to resolve this difficulty by the suggestion that a minor component of the interstellar grains in the form of graphite could form in stellar atmospheres and was sufficiently anisotropic in its optical properties as to provide adequate polarization. This suggestion was not pursued until somewhat later (Hoyle and Wickramasinghe, 1962). At about this time it was shown (Greenberg *et al.*, 1963a, 1963b) that given a sufficient degree of particle alignment, the dielectric ice grains of non-exotic shape would be quite adequate to provide the observed degrees of polarization. The concept of

F. J. Kerr and S. C. Simonson, III (eds.), Galactic Radio Astronomy, 155–177. All Rights Reserved.

grain production in stellar atmospheres led others (Kamijo, 1963) to the conclusion that silicates could be injected into space and perhaps constitute a major constituent of the grains.

The reasons why so many different materials with such a wide range of optical properties could be used to explain the extinction and polarization were that the free parameters defining the size distribution were sufficient to explain the available observational results which spanned the somewhat limited wavelength region from the near infrared to the near ultraviolet.

As data has accumulated in the far infrared and the far ultraviolet, the situation would be assumed to become clearer. However, even now, it is only possible by combining a wide range of observational and theoretical calculations and inferences to draw a reasonably consistent picture of grains. In the next section we shall summarize what we consider to be the key observational and theoretical criteria for determining the principal chemical composition. The subsequent sections will use these data to give a self-consistent picture of the grains which is then used to infer a particular grain model. This is not expected to be unique, but it appears to contain the most essential chemical ingredients in configurations which seem to follow from entirely separate considerations such as the distribution of dust in spiral galaxies.

II. Basic Observations and Interpretations

(a) WAVELENGTH DEPENDENCE OF EXTINCTION AND POLARIZATION

The wavelength dependence of the extinction and polarization provide the means of determining the typical sizes of the interstellar grains as dependent on the particular optical material of the chosen model. Thus it is simply demonstrated from a comparison of the average wavelength of the maximum polarization and the wavelength dependence of the polarization produced by aligned infinite cylinders of index of refraction $m = 1.33$ that a characteristic particle with this optical property should have a radius of about 0.15 μm (Greenberg, 1973c). Detailed considerations confirm this. For the purposes of this paper we refer to the wavelength dependence of extinction primarily for inferences on particle sizes.

In Figure 1 is shown a schematic representation of the extinction curve from $\lambda^{-1} = 0$ to $\lambda^{-1} = 10\ \mu\text{m}^{-1}$. Curves of this type have been obtained from OAO data (Bless and Savage, 1972) as well as from Copernicus (York *et al.*, 1973). The general character of the extinction curve seems to divide itself into three regions. The region from $1\ \mu\text{m}^{-1} \leqslant \lambda^{-1} \leqslant 3\ \mu\text{m}^{-1}$ has been well established for many years and henceforth we call it the 'classical' region. The extinction over this wavelength range is characterized by the same-sized particles as those producing the polarization maximum at about $\lambda^{-1} = 1.8\ \mu\text{m}^{-1}$. Excluding all other contributions to the extinction we would expect to see the extinction leveling off as shown by curve '2' in Figure 1. The continued rise in the extinction beyond $\lambda^{-1} \simeq 6\ \mu\text{m}^{-1}$ and, as indicated by the Copernicus results, even beyond $\lambda^{-1} = 10\ \mu\text{m}^{-1}$ can only be produced by solid particles whose sizes are characterized by radii of the order of or less than 10^{-6} cm (Greenberg, 1973a. 1973b).

These particles are associated with the curve '4'. The hump at $\lambda^{-1}=4.6\ \mu m^{-1}$ has been variously ascribed to graphite (Gilra, 1971) or silicates (Huffman and Stapp, 1971). The graphite particles needed to produce this feature are of sizes similar to those required to produce curve '4' and may indeed be the same particles. In the succeding

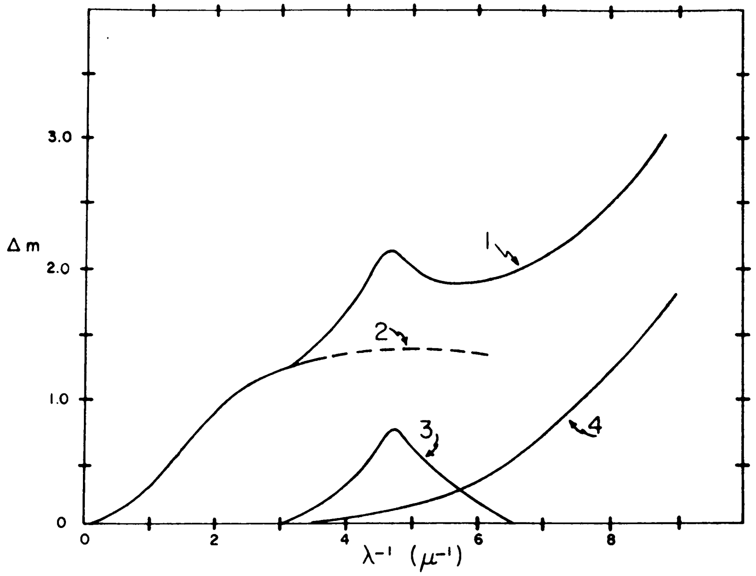

Fig. 1. Representative extinction curve and schematic separation into several contributions. Curves are labeled as follows: (1) Typical OAO extinction curve, (2) Dashed extension showing contribution by classical sized particles (as discussed in text), (3) Contribution of absorption in the 0.22 μm band, (4) Contribution by very small particles.

discussions the possibility that curve '4' is produced by either silicates or carbon will be taken up along with several other materials.

(b) TOTAL EXTINCTION

Unless otherwise stated, by the term total extinction we will mean the total *visual* extinction. In combination with a knowledge of the particle sizes and composition, the total extinction provides estimates of the solid particle contribution to the mass distribution in space. The following calculation of grain mass uses a spherical grain model. It will be shown later that this idealized representation does not modify the conclusion qualitatively because the effect of shape on the mass estimation is not significant.

A canonical value for the average extinction per unit distance is generally stated as

$$\Delta m_v/D = 2 \text{ mag kpc}^{-1}. \tag{1}$$

The average mass density of interstellar particles of a characteristic size (radius) $\bar{a}$

https://doi.org/10.1017/S0074180900026395 Published online by Cambridge University Press

and specific density s may be shown to be given by (Greenberg, 1968)

$$\varrho_{\mathrm{d}}=\tfrac{4}{3}\bar{a}s\Delta m/D, \tag{2}$$

where we implicitly assume that the extinction is produced primarily by the particles of effective size $\bar{a}$. As already noted, contributions to the extinction in other spectral regions are typified by other particle sizes. For $\Delta m_{\mathrm{v}}/D=2$ mag kpc $^{-1}$, Equation (2) gives

$$\varrho_{\mathrm{d}}=0.80\times10^{-21}\,\bar{a}s\ \mathrm{g\,cm^{-3}}, \tag{3}$$

Let $\bar{M}$ be the average molecular weight of the grain material and n_M be the number density of such molecules derived from Equation (3). From $n_M=\varrho_{\mathrm{d}}/\bar{M}m_{\mathrm{H}}$, where m_{H} is the atomic mass unit, we obtain

$$n_M=0.048\,\bar{a}s/\bar{M}. \tag{4}$$

It should be noted that a homogeneous dirty-ice grain model ($s=1$) with $\bar{a}=0.2\ \mu$m gives a ratio of gas-to-dust density of 100 for an average number density of hydrogen atoms $n_{\mathrm{H}}=1\ \mathrm{cm}^{-3}$. This value of n_{H} will be used throughout as the basic reference for defining the ratio n_M/n_{H} from which relative atomic abundances are obtained.

In deriving Equations (2) and (3) we have used the fact that at the wavelength of evaluation of the total extinction the individual particles extinction efficiences are $Q=C_{\mathrm{ext}}/\pi a^2\simeq1$, which gives (Greenberg, 1968)

$$\Delta m=1.086\,n_{\mathrm{d}}\pi\bar{a}^2D, \tag{5}$$

where n_{d} is the number density of grains.

(c) EFFECT OF SHAPE ON THE MASS ESTIMATION

Suppose we had considered truncated circular cylinders of radius a and length $2\varepsilon a$ (ε = length/diameter). Would this have affected the mass estimate significantly? The answer lies in evaluating the relative extinction per unit mass (or volume) for varying elongation.

It may be readily shown that the average projected area of an arbitrarily oriented convex particle is equal to one-fourth of the total surface area. Thus for an average extinction efficiency of $\bar{Q}$ we obtain the extinction averaged over orientation to be

$$C=\bar{Q}S/4,$$

where S = particle surface area. For a sphere and $\bar{Q}=1$ this reduces to $\bar{C}=\pi a^2$. The surface-to-volume ratio for the cylinders is

$$S/V=(1+2\varepsilon)/a\varepsilon, \tag{6}$$

from which we see that the change in the mass estimate using the *same* value of a is only about 17% in going from $\varepsilon=1$ to $\varepsilon=2$ and is only about 50% in going to $\varepsilon=\infty$! In view of the fact that the effective cylinder radius needed to produce the same wavelength dependence of the extinction as the spheres is less by perhaps 20% (Greenberg, 1968), we may infer that the net *overall* modification is largely cancelled; i.e., as ε increases we should decrease the value of a in Equation (6), thus leading to an almost invariant value of S/V. This general result is independent of the particular nonspherical shape chosen (Greenberg, 1973c, 1960). The detailed exact calculations will be presented in a later paper (Greenberg and Hong, 1974a).

(d) CIRCULAR POLARIZATION AND THE RATIO OF POLARIZATION TO EXTINCTION

The wavelength dependence of linear polarization gives no more definitive answer to the question of whether the grains are metallic or dielectric than does the extinction. However, recently the important discovery of the wavelength dependence of interstellar circular polarization (Kemp, 1973; Martin *et al.*, 1973) and its theoretical interpretation as being due to the birefringence of the interstellar medium created by aligned particles leads strongly to the conclusion that the grains which produce the linear polarization must be essentially dielectric (Martin, 1973). Metallic grains such as graphite are thus excluded as contributing substantially to the linear polarization.

The maximum ratio of polarization to extinction $\Delta m_p/\Delta m \simeq 0.06$ may be used to show that the major portion of the grains which produce the polarization must also be producing the extinction in the classical portion of the extinction curve unless we permit exceptional degrees of alignment. Let us assume that the visual extinction is produced partly by a non-polarizing component NP and partly by a polarizing component P. The ratio of polarization to extinction requirement is then (in optical depths rather than magnitudes) (Greenberg, 1969)

$$\frac{2(\tau_1^P - \tau_2^P)}{\tau^{NP} + (\tau_1^P + \tau_2^P)} = 0.06. \tag{7}$$

If we consider magnetic alignment, we find that even with field strengths as large as 10^{-5} G in clouds of density $n_H = 10\ \mathrm{cm}^{-3}$ and temperature $T = 100\,\mathrm{K}$ the best attainable value of $2(\tau_1^P - \tau_2^P)/(\tau_1^P + \tau_2^P)$ is *less* than about 0.08 even when *perfect* spinning alignment of the particles gives a ratio of polarization to extinction of 0.4 (the value for the core-mantle model discussed later). Thus Equation (7) gives $0.08/[(\tau^{NP}/\tau^P) + 1] = 0.06$, which allows a nonpolarizing contribution to the total extinction of $< 1/4$. In general, we conclude that certainly most of the particles producing the visual extinction are dielectric, although we can not exclude on this argument alone a contribution by metallic non-polarizing particles of perhaps 10–20%.

(e) INFRARED SPECTRA

The only direct spectral information on the chemical composition of the grains occurs in the infrared. The 0.22-μm hump (curve '3' in Figure 1) is not considered to provide as direct information. In general, the implication of a silicate component in circumstellar regions and in interstellar space depends on a broad feature of emission and absorption, respectively, centered around 9.7 μm. The search for a 3.07-μm absorption band in H_2O ice is extremely difficult and there is only one case in which both the

9.7-μm and 3.07-μm have been found to be simultaneously present. Figure 2, taken from Gillett and Forrest (1973), gives the basic datum which we use as a starting point in inferring that at least some ice is present in the interstellar medium.

We may calculate the relative volumes of ice and silicate material implied from the relative absorptions at 3.07 μm and 9.7 μm shown as essentially equal in Figure 2. If we base our result on the relative absorptivities of small separate spheres of ice and

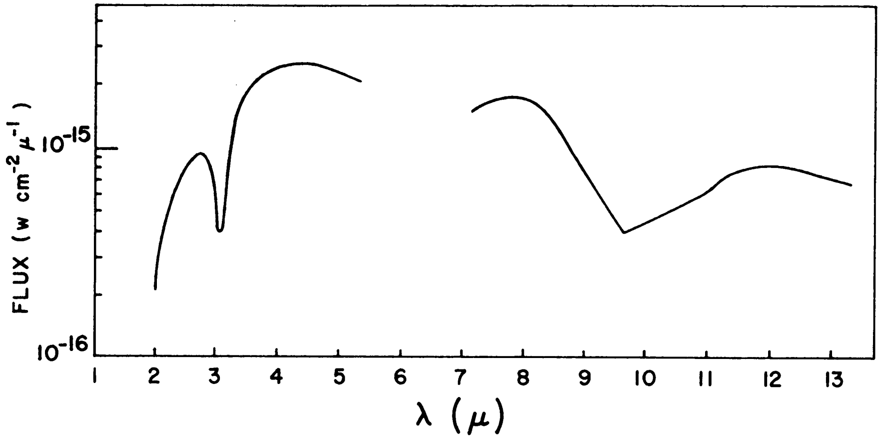

Fig. 2. Infrared spectrum of the Becklin-Neugebauer object. Adapted from Gillett and Forrest (1973).

silicate and using the obvious fact that $a/\lambda \ll 1$ in both cases, we arrive at a ratio $V_{ice}/V_{sil} = 0.21$ (Greenberg, 1973c). The assumption of *independent* particles of silicates and ices is probably unrealistic and may in some conditions produce spurious results. The condition under which the independent particle model gives reliable or incorrect results will be discussed later in some detail. At this point all that we wish to demonstrate is that: (1) both silicates and ice may be presumed to exist, and (2) the relative proportion of ice to silicate is *at least* 0.21. This value may be taken to be a lower bound if we generalize our definition of ice to include besides frozen H_2O various combinations of O, C N, and H as molecules and frozen free radicals. This has been justified on the basis of theoretical and experimental studies of the effects of ultraviolet irradiation of the grains (Greenberg, 1973c).

(f) COSMIC ABUNDANCE

The principal argument in this paper is based on a comparison between the abundances of various elements relative to hydrogen which would be demanded by postulated grain models and the cosmic abundance ratios which are presumed. For reference, Table I is abstracted from the latest compilation (Cameron, 1973).

III. Chemical Composition

In this section we shall compare a variety of interstellar grain models with respect to their relative compatibility with the cosmic abundances of Table I. We consider first

TABLE I

Selected abundances of the elements

Element	Relative number of atoms
H	1
C	3.70×10^{-4}
N	1.17×10^{-4}
O	6.76×10^{-4}
Mg	0.34×10^{-4}
Si	0.32×10^{-4}
Fe	0.26×10^{-4}

models for grains which produce the classical portion of the extinction curve labeled '2' because, as will appear later, these particles contain most of the mass.

(a) HOMOGENEOUS MODELS

Even though the assumption of a single chemical component to represent the interstellar grains is not realistic, it serves as a very useful starting point in defining the limitations imposed by chemical abundances. The representative sizes selected for each material are based only on the broadest characteristics of curve '2'; i.e., we attempt only to match approximately the single particle position of extinction saturation with the value $\lambda^{-1} \simeq 4\ \mu m^{-1}$ in curve '2'. Table II summarizes the results for a number of grain ingredients.

We see from Table II that the only grain ingredients which fit comfortably on cosmic

TABLE II

Atomic densities for homogeneous grain models
$\Delta m/D = 2$ mag kpc^{-1}, $n_H = 1$ cm^{-3}, $\bar{Q} = 1$[d]

Material	$\bar{M}$	$\bar{a}$ (μm)	$\bar{s}$	n_M (cm^{-3})	$\frac{[O]}{[H]}$	$\frac{[Si]}{[H]}$	$\frac{[Mg, Fe]}{[H]}$	$\frac{[Fe]}{[H]}$	$\frac{[C]}{[H]}$
					$\times 10^{-4}$				
'Ice'	17	0.2	1.0	5.61	3.28[a]				1.80
Orthopyroxene[b]	116	0.1	3.6	1.48	4.44	1.48	1.48		
Olivine[c]	172	0.1	3.8	1.05	4.20	1.05	2.10		
Magnetite	232	0.05	6.0	0.62	2.47			1.86	
Iron	56	0.05	7.9	3.36				3.36	
Silicon Carbide	38	0.05	3.2	2.02		2.02			2.02
Carbon	12	0.05	2.2	4.40					4.40
Cosmic Abundance					6.76	0.32	(Mg)0.34	0.26	3.70

[a] 3.28 is reduced from 5.61 because 'Ice' means [O, C, N] in relative cosmic abundances; i.e., O:C:N = 6.76:3.70:1.17 comprising a variety of complex organic molecules and frozen free radicals.
[b] Orthopyroxene = (Mg, Fe) SiO_3.
[c] Olivine = $(Mg, Fe)_2\ SiO_4$.
[d] For metals (magnetite, iron, carbon) the appropriate $\bar{Q}$ value is about 1.3 and for dielectrics $\bar{Q} \approx 1.5$. The last six columns of the table should be divided by these factors.

https://doi.org/10.1017/S0074180900026395 Published online by Cambridge University Press

abundance arguments are the dirty ice model and possibly the carbon which is discrepant only by a factor of two. All others produce discordant abundances by factors of at least 4. Thus, while orthopyroxene requires only about twice the CA amount of Mg and Fe it requires six times the CA of silicon and this is a fairly severe restriction. (These factors of rejection are reduced by using $\bar{Q}>1$ but not by enough to change the conclusions.) It would appear that SiC is precluded from providing a major portion of the visual extinction as would seem to be required by some grain models (Gilra, 1971). The carbon must be excluded as a major constituent primarily because of the presumed dielectric optical properties of the grains producing visual extinction and polarization. Note that we have yet to add a grain component to give the far ultraviolet extinction.

(b) CORE-MANTLE PARTICLES – CLASSICAL EXTINCTION

It seems highly unlikely that if silicates and ices are present in space they occur as disconnected objects. The most reasonable way for ice to form in interstellar space is by accretion on some nucleation points. We therefore assume that silicates and ices appear as cores and mantles respectively. Other materials may also provide cores but at this time we restrict ourselves to silicate cores alone for the classical particles. A summary picture of possible processes leading to this model is presented later.

In the following discussion the particles are treated as concentric spheres. The results for a more detailed model using concentric cylinders are given later and compared directly with observations.

Let a_c and a_m be the core and mantle radii respectively, and let $\alpha = a_m/a_c$. Again, letting $Q=1$, Equation (5) is replaced by

$$\Delta m = 1.086\, n_d \pi a_m^2 D\,, \tag{8}$$

from which we obtain

$$\varrho_c = \frac{4}{3}\frac{a_m s}{\alpha^3}\,\frac{\Delta m}{1.086D} = 0.80 \times 10^{-21}(a_m s/\alpha^3), \qquad (\Delta m/D = 2 \text{ mag kpc}^{-1}), \tag{9}$$

where ϱ_c means space density of the core material only.
Based on the concentric cylinder model we choose $a_c = 0.08\ \mu$m and find that in order to bring the [Si]/[H] ratio down to its CA level we must have approximately $\alpha = 1.8$, neglecting the possible contribution of the very small particles which are considered in the next section. This means that the value of $V_{\text{'ice'}}/V_{\text{sil}}$ must be closer to 0.8 than the 0.2 derived directly from the Becklin-Neugebauer object for H_2O ice. It should be kept in mind that the choice of $a_c = 0.08\ \mu$m is probably not unique and may, indeed, not even be the best value. It was determined in an essentially empirical fashion based on 'cut and try' calculations on a few concentric cylinder models.

(c) VERY SMALL PARTICLES – FAR-ULTRAVIOLET EXTINCTION

As is well-known, the classical-sized particles can not produce the shape of the far ultraviolet extinction curve '4'. It is not at all unusual to find the extinction at 1000 Å

($\lambda^{-1} = 10\ \mu\text{m}^{-1}$) to be perhaps 3 or 4 times larger than the visual extinction. In the following calculations we let $\Delta m(10) = 4\Delta m_v$. Then the contribution of the small particles alone to the extinction at $\lambda^{-1} = 10\ \mu\text{m}^{-1}$ is $4\Delta m_v - 2\Delta m_v = 2\Delta m_v$ where we have used the approximate result that the saturation extinction by the classical particles is twice the visual extinction. We thus have

$$\begin{aligned} \varrho_b &= 0.40 \times 10^{-21} a_b s\ \frac{2\Delta m_v}{D} \\ &= 1.6 \times 10^{-21} a_b s \qquad (\Delta m_v/D = 2\ \text{mag kpc}^{-1}), \\ n_M &= 0.095\ a_b s/\bar{M}, \end{aligned} \tag{10}$$

where a_b is the radius of the very small particles assumed to be *bare* for reasons which will be demonstrated later and where ϱ_b = space density of the bare particles.

Using $a_b = 0.01\ \mu$m we have the results shown in Table III.

TABLE III

Abundances for bare particles

Material	n_M (cm^{-3})	$\frac{[Si]}{[H]}$		$\frac{[Fe, Mg]}{[H]}$ $\times 10^{-4}$	$\frac{[Fe]}{[H]}$	$\frac{[C]}{[H]}$
Orthopyroxene	0.295	0.295		0.295		
Olivine	0.210	0.210		0.420		
Magnetite	0.246				0.738	
Iron	1.34				1.34	
Carbon	1.74					1.74
Silicon Carbide	0.80	0.80				0.80
Cosmic Abundance		0.32	(Mg)	0.34	0.26	3.70

We note immediately that the contribution of the very small particles to the heavy element mass is comparable with that of the cores. However, we must keep in mind that our particle parameters are only chosen on a semi-quantitative basis so that factors of two may not be sufficient to exclude a model. On the other hand, factors of 4 or more must be taken seriously. In any case, there is abundant evidence from the above arguments that most of the heavy elements in interstellar space must be bound up in the form of solid particles. This is particularly true of the Si, Fe, Mg group, and to a lesser extent for O, N, C. These results appear to be compatible with the observed depletion (Morton *et al.*, 1973; Rogerson *et al.*, 1973). An additional depletion of C relative to O and N, which has been reported, could be attributed to the existence of very small graphite particles required for producing the 0.22-μm absorption hump.

It appears that iron particles may contribute no more than about 10% of the far ultraviolet extinction. Magnetite also is not an important constituent.

Incidentally, none of the above arguments exclude any heavy-element constituent from being part of the grain-core population but merely excludes them from providing the major optical manifestations of interstellar grains.

We conclude that cosmic-abundance arguments lead us to require the major optical effects of grains in the classical region to be produced by the mantles and the major additional effects in the far-ultraviolet to be produced by very small uncoated particles whose chemical composition is primarily silicate and/or carbon with the 0.22-μm hump leaning to support of the latter.

(d) RELATIVE NUMBERS OF CORE-MANTLES AND BARE PARTICLES

The number of grains is a rather artificial concept because it is usually based on the assumption of a single representative particle size. Nevertheless, it is a useful working model so long as one does not apply it without appropriate reservations.

The typical extinction values in the visible and far-ultraviolet, as defined in Sections IIIb and IIIc respectively, result in the number of core-mantle, n_{C-M}, and the number of bare particles n_b being given by

$$n_{C-M} = 1.3 \times 10^{-12}\ \mathrm{cm}^{-3}, \qquad \Delta m_v/D = 2\ \mathrm{mag\ kpc}^{-1}$$
$$n_b = 290\, n_{C-M}, \qquad \Delta m_{10} = 4\Delta m_v,$$

where the core radius is given by $a_c = 0.08\ \mu$m, the ratio of mantle to core radius is $\alpha = 1.5$, and the bare particle radius is $a_b = 0.01\ \mu$m.

IV. Small-Particle Temperatures

One of the properties of small grains which may at first be thought to provide a condition for distinguishing between the accretion possibilities of the core particles and the much smaller 'bare' particles is the fact that, in general, the temperatures of small particles increase with decreasing size. We see in the next section that this effect is not large enough to be particularly important. In the subsequent section, however, we show that the very small size of the bare particle leads to another phenomenon associated with radiant energy absorption; namely, energy fluctuations which are significantly larger than the average energy content of the grains and it is this effect which is presumed to be the agency for inhibiting accretion.

(a) EQUILIBRIUM TEMPERATURES

It has long been recognized that very small particles immersed in the interstellar radiation field arrive at equilibrium temperatures substantially higher than those of a black body (van de Hulst, 1946). The reason for this is apparent from elementary considerations of the equation relating the particle radiation absorption to emission.

$$\int_0^\infty \varepsilon_{ab}(a, \lambda)\, R(\lambda)\, d\lambda = \int_0^\infty \varepsilon_{em}(a, \lambda)\, B(\lambda, T_d)\, d\lambda$$

or

$$\bar{\varepsilon}_{ab} \int_0^\infty R(\lambda)\, d\lambda = \bar{\varepsilon}_{em} \int_0^\infty B(\lambda, T_d)\, d\lambda,$$

where ε_{ab} and ε_{em} are the wavelength-dependent absorption efficiencies of the particles of size a, $R(\lambda)$ is the interstellar radiation field, and $B(\lambda, T_d)$ is the Planck function for the grain temperature T_d. It is convenient to consider Equation (11) in terms of average efficiencies $\bar{\varepsilon}_{ab}$ and $\bar{\varepsilon}_{em}$. Further, to arrive at a size dependence it is useful to let $\bar{\varepsilon}_{em} = \bar{\varepsilon}_{eff} = 33.3aT_d$, which will give a lower bound on the particle temperatures (Greenberg, 1971) because it is defined by maximum particle emissivity. The values of ε are strongly dependent on the value of a/λ, approaching unity as $a/\lambda \to \infty$ and zero as $a/\lambda \to 0$. Since the radiation is generally absorbed at values of λ for which a/λ is much larger than its value at the important emission regions, we find that the temperature T_d defined by Equation (11) is higher than the black-body temperature. For example we note that, for an 'ice' particle, $\bar{\varepsilon}_{ab} = 0.1$ for $a = 0.1$ μm and $\bar{\varepsilon}_{ab} = 1.0$ for $a = 1.0$ μm if the interstellar radiation field is represented by $R(\lambda) = WT^4$, with $W = 10^{-14}$ and $T = 10000$ K (Greenberg, 1968). Using the maximum long-wavelength emissivity, ε_{eff}, we get $T_d = 8$ K for the 0.1-μm particle which is only about 3 K less than a more correctly obtained value. We should not be surprised to find that a 0.01-μm (10^{-6} cm) particle does not become significantly hotter when we realize that while $\bar{\varepsilon}_{em}$ is decreasing with size, so also is $\bar{\varepsilon}_{ab}$. This may be shown by extrapolation of the curves showing the variation of grain temperature with size (Greenberg, 1968). Thus the very small particles referred to earlier as bare particles differ little in temperature from the classical-sized cores, and consequently this alone can not provide a reason for the bare particles remaining bare.

(b) TEMPERATURE FLUCTUATION OF BARE PARTICLES

It has been mentioned (Greenberg, 1968) that the concept of grain equilibrium temperature is meaningful only when the rate of energy input per second from the radiation field is generally very small compared to the average total energy content of the grain. This condition is fulfilled for the grains larger than 0.05 μm in radius. For sufficiently small grains it was shown that this condition is not met.

The energy content of a grain is given by (Kittel, 1956)

$$U = \frac{3\pi^4}{5} NkT_d (T_d/\theta)^3, \tag{12}$$

where N = number of atoms per cm^3 and θ = Debye temperature. This, of course, is the result for a reasonably defined solid and therefore we must assume that the bare particles are of this character. The value of N in Equation (12) is obtained from

$$N = \frac{4}{3} \frac{\pi a^3 s}{\bar{M} m_H}; \tag{13}$$

665 K is used for the Debye temperature of olivine and 420 K for that of graphite. The value of 696 K for orthopyroxene is so close to that of olivine that the latter serves to give an adequate illustration of the temperature fluctuation for silicates. Graphite is a two dimensional lattice with a more complicated low temperature spe-

cific heat. Our use of a T^3 law with an effective Debye temperature is approximate and probably underestimates the temperature fluctuations.

In Figures 3 and 4 the ratio of the final temperature, after absorbing energy $h\nu$, to the equilibrium dust temperature $T_f/T_d = [(U+h\nu)/U]^{1/4}$ is plotted against the energy of the absorbed photon in olivine and graphite particles. With the Equations (12) and (13) this ratio is given by

$$\frac{T_f}{T_d} = \left(1 + \frac{5\bar{M} m_H \theta^3 h\nu}{4\pi^5 ska^3 T_d^4}\right)^{1/4}. \tag{14}$$

Hence we see that the final temperature is roughly independent of the initial temperature which was taken as the equilibrium dust temperature, and that the final temperature is proportional to $a^{-3/4}$ as a approaches zero. We see, for example, that when a 0.01-μm olivine grain whose equilibrium temperature is either 5 or 10 K absorbs a 5-eV photon ($\lambda = 240$ nm) its temperature jumps to 46.5 K or 48 K respec-

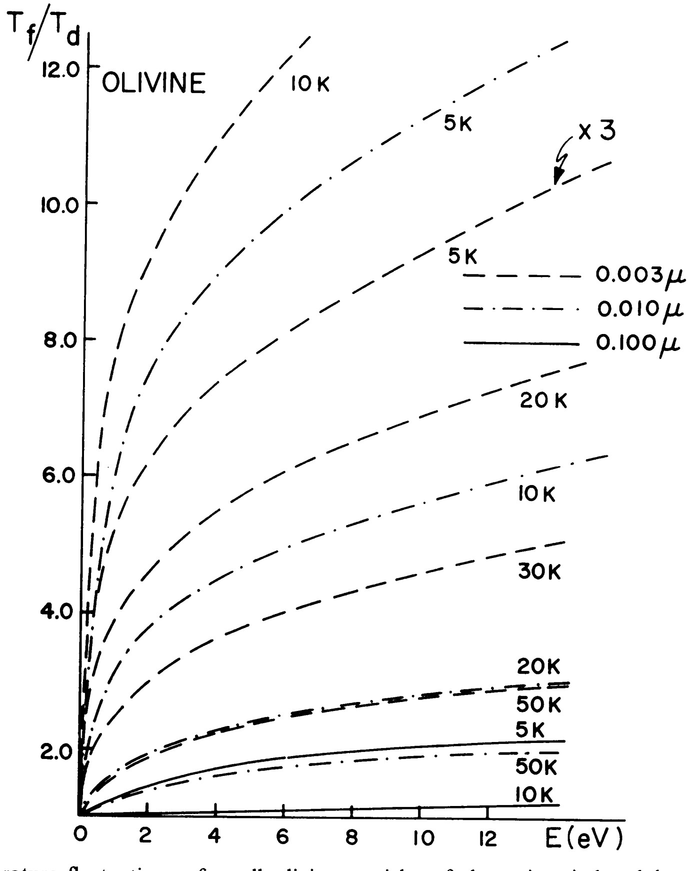

Fig. 3. Temperature fluctuations of small olivine particles of three sizes induced by single photon absorption. Each curve is labeled with its appropriate equilibrium temperature. As indicated the curve for $a = 0.003\ \mu$m and $T_d = 5$ K should be multiplied by a factor of three.

https://doi.org/10.1017/S0074180900026395 Published online by Cambridge University Press

tively, and that going from $a=0.01$ μm to $a=0.03$ μm the final temperature rises to approximately 150 K.

This is reminiscent of a remark made earlier (Greenberg, 1968) with regard to the temperature of Platt (1956) particles.

It seems reasonable to conclude that such temperatures are adequate to prevent accretion on the bare silicate particles if they are sufficiently small and in the size

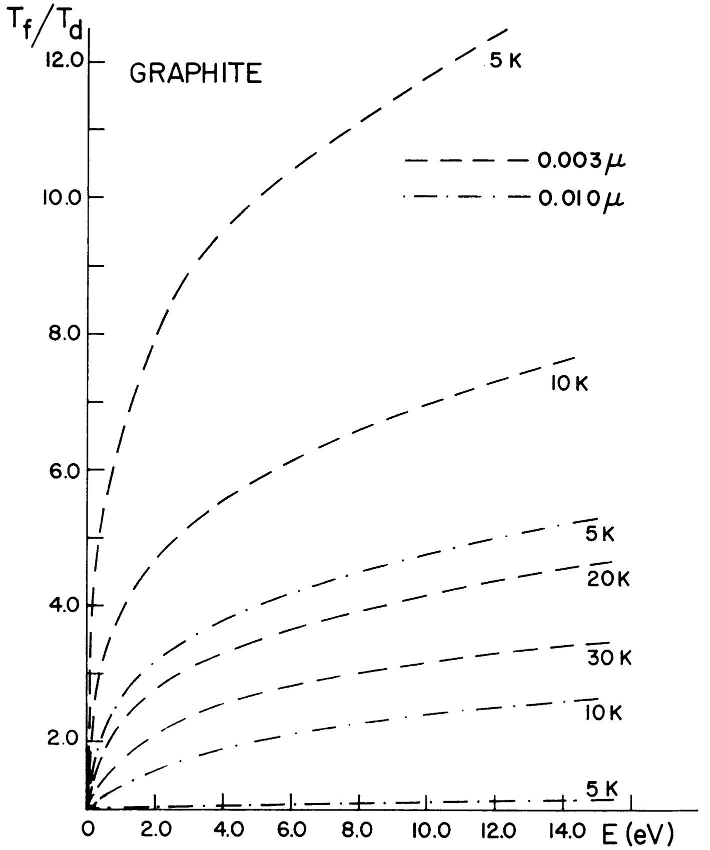

Fig. 4. Temperature fluctuations of small graphite particles of two sizes induced by single photon absorption. Each curve is labeled with its appropriate equilibrium temperature.

range required for the far ultraviolet extinction. The normal graphite temperatures are larger than the silicate temperatures; and their fluctuating values are somewhat more violent because graphite has a larger effective Debye temperature. Therefore this mechanism should play a similar role in inhibiting accretion in normal radiation fields.

V. Extinction to the Galactic Center

There are many reasons why the sizes of the mantles relative to the cores should be different from region to region in the Milky Way: different time scales for accretion due to the different physical conditions from place to place, possibilities for evaporation and sputtering, etc. It is by simultaneously measuring both the total extinction and the silicate band absorption that one may obtain such a measure most directly. As we shall see in the discussion of models, the variation of total-to-selective extinction is not a very sensitive discriminant of the mantle size over a wide range.

The silicate band absorption at 9.7 μm toward the galactic center is about $\Delta m_{9.7-\mu m}=3$ (Woolf, 1973). Using a value of $m_{sil}=1.7-0.71\,i$ leads to an extinction per unit volume of silicate core of $\Delta m_{9.7-\mu m}/V=0.609$. Thus from Equation (5) we get $\Delta m_V=4.06/\bar{a}$ for pure silicate grains of mean representative size $\bar{a}$ with no mantles. For $a=0.1$ μm this leads to $\Delta m_V=40.6$ or about 27, which seems generally in the range of the accepted value of 27 mag extinction to the center (Borgman, 1974). We note that if $\bar{a}$ is as much as 0.2, which has been occasionally used in the literature, the extinction would be only about 20 mag.

In order to evaluate the effect of mantles we borrow the core and mantle parameters from those which are used in our model calculations. We see in Table IV that consistent with the model parameters leading to essentially constant values of the ratio of total-to-selective extinction, there is a very wide range in possible values of the extinction to the galactic center. The equation for Δm_V is modified from the above to $\Delta m_V=4.1\,\alpha^2/a_1$ where α is the ratio of the mantle-to-core radii and a_1 is the core radius.

TABLE IV

Mantle size effect on extinction to galactic center
$a_1=0.08$ μm

a_2	α	Δm_V
0.1	1.25	98
0.12	1.50	113 (92)
0.20	2.50	312

The values for Δm_V given in Table IV are correct if we assume that the particles producing the far-ultraviolet extinction are either non-existent or consist of some material (like graphite) not composed of silicates. If there are small bare silicate particles the values of Δm_V are reduced accordingly so that, for example, if we use the number of bare particles implied by our typical extinction curve we would reduce the value 113 to 92 as shown in parentheses.

According to our model, then, a value of $\Delta m_V=41$ implies no mantles whatsoever on grains in the galactic center. It should be pointed out that more carefully calculated values of Q (the extinction efficiency) would modify our results somewhat and that such calculations are in progress. However, no significant changes in our conclusions are anticipated and if the value of $\Delta m_V=27$ is independently confirmed, the mantles on dust grains near the galactic center must be very thin.

VI. Core-Mantle Cylinder Model

We have chosen as representative of a class of core-mantle cylinder models the case in which all cores are the same radius, $a_c = 0.08$ μm, and the mantles are distributed in sizes according to the form $n(a_m) = \exp\{-5[(a_m - a_c)/a_i]^3\}$, where $a_i = 0.12$, 0.14, 0.16 μm. The average or effective single value of a_m has been shown to be given by $a_m - a_c \cong 0.3\, a_i$ Greenberg (1968). Single equivalent mantle thicknesses are respectively 0.036, 0.042, 0.048 μm, which give $a_m = 0.116$, 0.122, 0.128 μm.

In order to obtain a realistic value of the polarization, we have performed the calculations for spinning cylinders corresponding to perfect Davis-Greenstein orientation. The computer program for arbitrarily oriented cylinders has been generalized from that for homogeneous cylinders (Lind and Greenberg, 1969) to concentric core and mantle cylinders (Shah, 1970). The numerical calculations are performed to obtain the extinction from the total cross sections for orthogonal polarizations of the incident radiation,

$$C_E = \frac{2}{\pi} \int_{a_c}^{\infty} n(a_m)\, \mathrm{d}a_m \int_0^{\pi/2} C_E(a_c, a_m, \chi)\, \mathrm{d}\chi, \qquad (15)$$
$$C_H = \frac{2}{\pi} \int_{a_c}^{\infty} n(a_m)\, \mathrm{d}a_m \int_0^{\pi/2} C_H(a_c, a_m, \chi)\, \mathrm{d}\chi,$$

where χ is the tilt angle of the cylinder axis with respect to the direction of incident radiation. The integration intervals used were $\Delta a_m = 0.01$ and $\Delta\chi = 9°$.

The normalized extinction values of $\Delta m = [(C_E + C_H)/2]\ [\Delta m(1) = 0,\ \Delta m(3) = 1]$ for the three values of a_i are shown in Figure 5, where comparison in each case is made with the observations which have been obtained from appropriate renormalization of the data of Whiteoak (1966) and Bless and Savage (1972). Within the range $1 \leqslant \leqslant \lambda^{-1} \leqslant 3\ \mu\mathrm{m}^{-1}$ all three calculated curves are almost indistinguishable from each other and give an excellent reproduction of the observational results. The total variation in mantle thickness in the three models is a factor of about 1.5 and the variation in total thickness is about 10%. A most significant consequence of the core-mantle model therefore is the essential invariance of the extinction curve to variation in mantle thickness. This is quite different from the result for homogeneous particles (see for example the numerous cases presented by Greenberg (1968) as well as elsewhere) where a 20% change in size produces a large change in curvature of the extinction around $\lambda^{-1} = 2\ \mu\mathrm{m}^{-1}$.

The *general* uniformity of the shape of the extinction in the visual region with its concomitant constancy in the ratio of A_v/E_{B-V} has long represented a puzzle to those who wished to represent the grains by particles which accrete matter in space and are therefore of variable size depending on their history. The statistical growth-destruction calculation of Oort and van de Hulst (1946) answered the question but

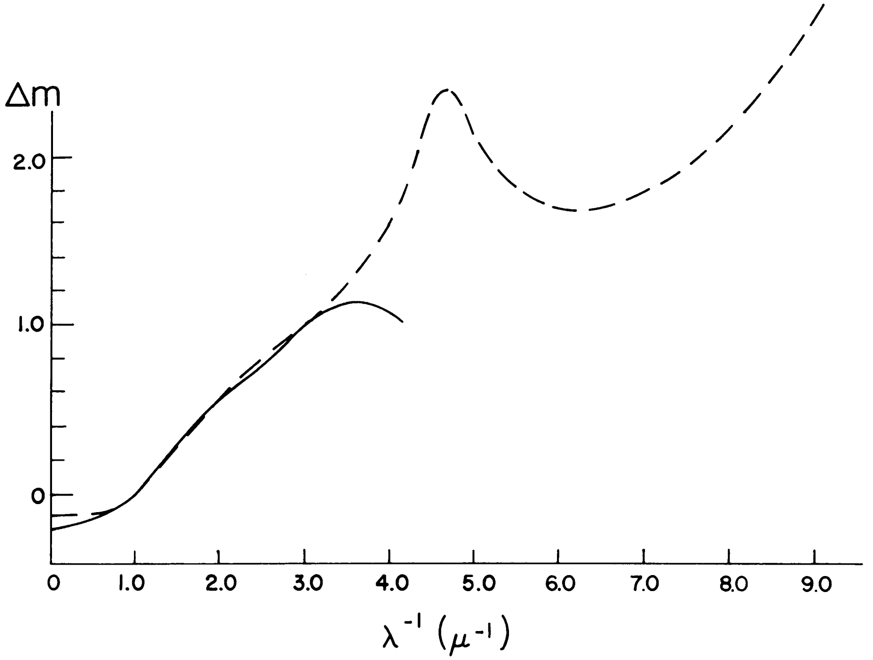

Figs. 5a–c. Comparison of calculated extinction by spinning core-mantle cylinders (solid curves) with observations (dashed curves). $R_{\rm obs} = 3.20$

Fig. 5a. $a_c = 0.08\ \mu$m, $n(a_m) = \exp\left[-5\left(\dfrac{a_m - 0.08}{0.12}\right)^3\right]$

$R_{\rm calc} = 3.19.$

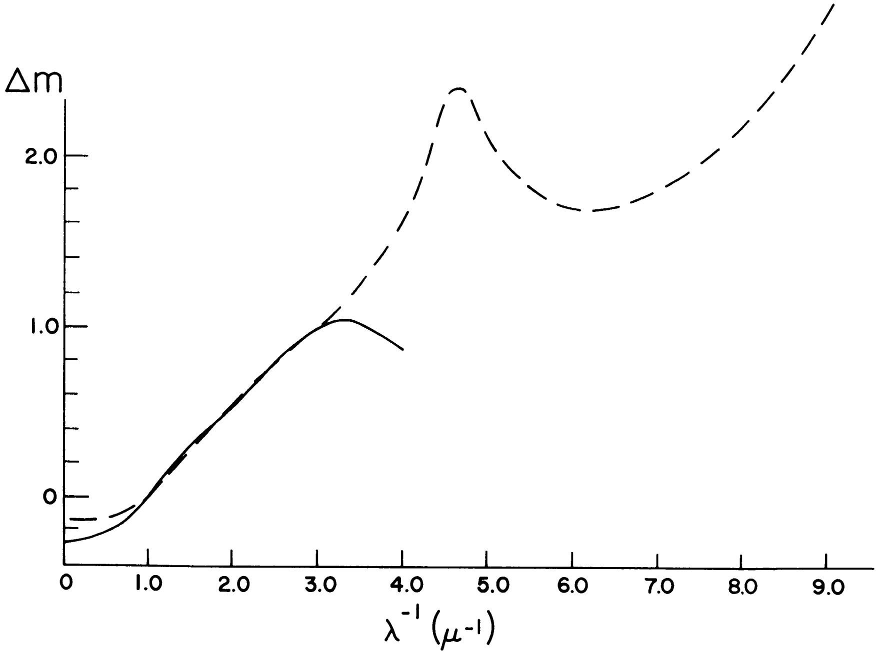

Fig. 5b. $a_c = 0.08\ \mu$m, $n(a_m) = \exp\left[-5\left(\dfrac{a_m - 0.08}{0.14}\right)^3\right]$

$R_{\rm calc} = 3.27.$

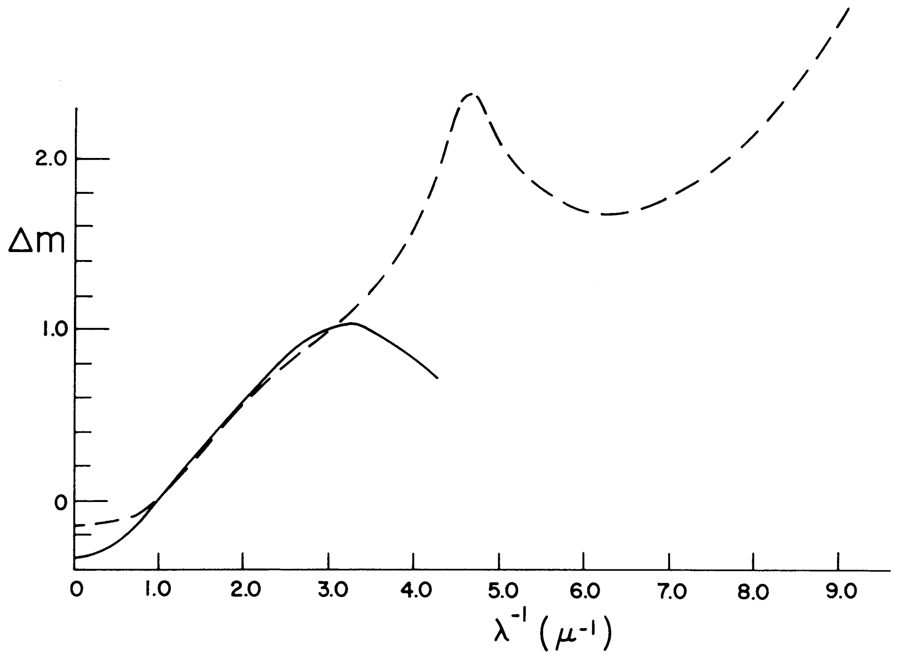

Fig. 5c. $a_c = 0.08\ \mu\text{m},\ n(a_m) = \exp\left[-5\left(\frac{a_m - 0.08}{0.16}\right)^3\right]$

$R_{calc} = 3.37.$

only on the basis of an *average* over many dust clouds. Even disregarding the question of validity of random cloud-cloud collisions providing the grain destruction mechanism it was still difficult to answer the question of why the ratio A/E varied so little (with some clear exceptions for which good theoretical grounds existed). It is thus satisfying to have a grain model which has the character of preserving the invariability of A_v/E_{B-V} over such a wide range of physical conditions and history as evidenced by large differences in mantle thickness.

(b) POLARIZATION

The polarization is obtained from $\Delta m_p \sim C_E - C_H$. The wavelength dependence of polarization and ratio of polarization to extinction are shown in Figure 6. The position of P_{max} is seen to shift toward lower values of λ^{-1} as a_i increases in just about the same way as would be expected for homogeneous particles. Thus the wavelength dependence of polarization is still a good discriminant of particle size. We note also that the ratio of polarization to extinction is significantly larger for the core-mantle particles which satisfy the extinction than for homogeneous particles. They will thus more readily produce the observed ratios of polarization to extinction for a *given* magnetic field. In addition, because they are smaller in outer dimension, their inertial properties are better (lower moment of inertia) for orientation.

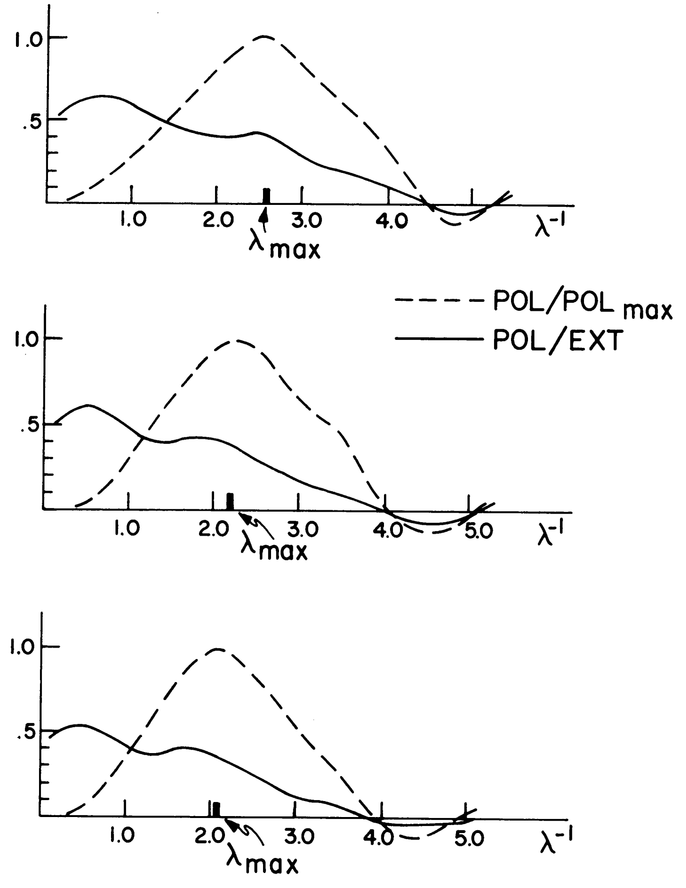

Fig. 6. Calculated wavelength dependence of polarization and ratio of polarization to extinction by spinning core-mantle cylinders. Upper figure corresponds to Figure 5a; middle corresponds to Figure 5b; bottom corresponds to Figure 5c.

(c) IR ABSORPTION ESTIMATES

One factor which has not hitherto been seriously considered in interpretation of infrared absorption bands is that these bands are produced in a combination of one material imbedded in the other rather than in isolated particles of different materials. A preliminary calculation has been made for several combinations of absorptive properties of core and mantle materials in order to determine how important this effect may be in modifying estimates of core and mantle masses based on isolated particle calculations.

Even when the mantle has no absorption at the position of the core absorption band there is some deviation – although not great; similarly when the roles are reversed. If, however, the mantle material has absorption in the vicinity of the core absorption, then the interpretation of the core mass (volume) based on the extinction will be significantly altered. Clearly an absorbing mantle hides the core. A proper calculation of this effect would have to be performed over the full extent of the absorption band in order to see not only the modification on the depth but also the shape of the band. Such calculations are in progress for selected core and mantle materials. However, as an indication of the magnitude of what to expect we present in Table V the volume of material inferred from the depth of an absorption band produced by a core-mantle particle compared with that which would be given by the *actual* volume of the core or mantle material if it occurred in isolated spherical

TABLE V

Ratios of estimated to actual volumes of core and mantle materials based on absorption band depths

Sphere	I		II		III		IV	
α	sil	ice	sil	ice	sil	ice	sil	ice
1.12	1.076	0.817	1.016	0.817	1.076	0.846	1.016	0.846
1.25	1.164	0.865	1.023	0.865	1.164	0.879	1.023	0.879
1.50	1.396	0.921	1.026	0.912	1.396	0.928	1.026	0.928
2.00	2.151	0.967	1.028	0.967	2.151	0.969	1.023	0.969
2.50	3.400	0.982	1.033	0.982	3.400	0.984	1.033	0.984
Cylinder								
1.12	1.057	0.998	1.013	0.998	1.057	1.051	1.013	1.051
1.25	1.121	0.992	1.026	0.992	1.121	1.017	1.025	1.017
1.50	1.271	0.996	1.054	0.996	1.271	1.008	1.054	1.008
2.00	1.679	0.997	1.140	0.997	1.679	1.002	1.140	1.002
2.50	2.264	0.990	1.296	0.990	2.264	0.992	1.296	0.992

	sil	ice		dark	clear
I	clear	dark	$m_{\text{sil}}(10) = 1.52-$	$i\,0.68$	
II	clear	clear	$m_{\text{ice}}(3.1) = 1.375-$	$i\,0.815$	
III	dark	dark	$m_{\text{sil}}(3.1) = 1.6-$	$i\,0.01$ or	1.6
IV	dark	clear	$m_{\text{ice}}(10) = 1.6-$	$i\,0.115$ or	1.6

Dark and clear refer to absorbing or non-absorbing representations of silicate and ice materials.

or cylindrical particles. It appears clear that if the mantle 'ice' were actual ice (solid H_2O) the silicate core 9.7-μm absorption would be almost entirely masked by the mantle absorption and any estimates of silicate mass based on it would be overestimated by 30% (cylinder) to 40% (sphere) even when the mantle is only half as thick as the core. Since we do not really know the absorption spectrum of the mantle composition, we should not overinterpret this result. It is to be remembered that it is so only as a possibility. Experiments are planned to measure the infrared absorption properties of ultraviolet irradiated dirty ice at low temperatures using experimental methods which have been reported earlier (Greenberg, 1973b).

VII. Variability of Grain Characteristics with Distribution

The core-mantle plus bare particle model for the grains leads to a number of iden-

https://doi.org/10.1017/S0074180900026395 Published online by Cambridge University Press

tifiable changes which may be expected in the physical – and observational – characteristics of the grains as they go through various stages in their development. For this paper we will introduce and briefly discuss the kinds of changes in the grains which are particularly an outcome of this model. Detailed considerations are deferred to a later paper.

(a) THE INTERARM REGION

Let us suppose, following the general scheme outlined by Greenberg (1970), that, as the gas and accompanying grains pass through the outer edge of the density-wave spiral arm, they are of 'normal' composition and size distribution, i.e., the relative number of core-mantle and bare particles is as defined in Section IIId. We expect sputtering of the mantles to begin to take place as a consequence of the He and H atom bombardment (H atoms are less effective because of their mass) at temperatures greater than 1000 K.

If P_{sp} is the probability that the average colliding He atom causes a molecule of molecular weight M_{mol} to be sputtered off, the rate of decrease of the radius of the grain is

$$\dot{a} = -P_{sp} \frac{n_{He} v_{He} M_{mol} m_H}{4s}, \tag{16}$$

where n_{He} is the number density of He atoms, v_{He} is the average He atom velocity, and s is the specific gravity of the grain mantle material. Unfortunately, we do not know the sputtering rates with much reliability at the low energies corresponding to temperatures of 1000–10000 K. Furthermore, the chemical composition of the mantle is not precisely known except that it consists of *various* combinations of O, C, N, and H. If these combinations are predominantly of large molecular weight, results based on H_2O and CH_4 sputtering (Aannestad, 1973) would have to be revised. Finally, surface characteristics undoubtedly play a very important role in the sputtering process.

Low-energy-sputtering yield rates for H and He on solid H_2O and CH_4 have been given by Aannestad (1973). Greenberg (1973) used an average value of $\langle P_{sp} \rangle = 10^{-2}$ for H atom collisions in the 1000–10000 K range.

For $n_H = 0.2\ \text{cm}^{-3}$ ($n_{He} = 0.02\ \text{cm}^{-3}$), $\bar{v}_{He} = (\bar{T}/100)^{1/2}(0.8) \times 10^5\ \text{cm s}^{-1}$, $\bar{T} = 5000$ K, $M_{mol} = 20$, $s = 1$, we get

$$\dot{a}/P_{sp} = -9.4 \times 10^{-20}\ \text{cm s}^{-1} = 2.8 \times 10^{-6}\ \text{cm}\,(10^6\ \text{yr})^{-1}.$$

Thus taking P_{sp} typically as 10^{-1} we find that a mantle thickness of 0.05 μm is sputtered off in 17×10^6 yr. In the time it takes the grain to arrive at the inner edge of the next arm (10^8 yr) all mantles up to 0.28 μm thick (!) would be sputtered away. This is substantially greater than the maximum in the mantle thickness of 0.13 μm in the largest size distribution we have used to give a normal classical extinction for the core-mantle model. Therefore, if our estimate of the sputtering rate is reasonable – and this is yet to be firmly established – we expect that it is only silicate cores of the large grains and the small bare particles which survive the hostile interarm region.

An obvious observational consequence is that the ratio of the far-ultraviolet extinction to the visual extinction should be much larger than normal because the visual extinction per large grain is everywhere (in wavelength) decreased while the far-ultraviolet extinction by the bare particles may be essentially constant. Thus estimates of the far-ultraviolet attenuation in the interarm region are greater than would be given by extrapolation from the E_{B-V} color excess.

(b) INNER EDGES OF ARMS

As the residual silicate cores arrive in the compression region of the inner edge of an arm they may be expected to accrete new mantles at a rate fast enough to provide a rather sharp discontinuity in the grain characteristics as seen in photographs of external galaxies (Lynds, 1970) and as discussed earlier (Greenberg, 1970). It should be pointed out here that a factor of $\frac{1}{4}$ was inadvertently omitted from Equation (6) of that paper, but the conclusions are the same.

(c) DARK CLOUDS

The dark clouds which are regions of very high dust and gas density contain substantial volumes of material which are well shielded from the interstellar radiation field. Consequently, we expect that the bare particles are not only at lower temperatures than normal (Greenberg, 1971) but more importantly their temperature fluctuations are greatly reduced in frequency. Under these conditions the bare particles become suitable nucleation points for accretion of the condensible gases. The total extinction increases but the relative amount of ultraviolet to visual extinction decreases. For example, the rate of accretion of mantles in a medium with gas density of (O + C + N) of 10 – corresponding to a number density of H atoms (free or bound) of 10^4 – would be sufficient to produce 'ice' mantles of 0.05 μm in thickness in about 5×10^4 yr. This time is shorter than the collapse time of such a typical dark cloud. With such particles the saturation extinction would be at about $\lambda^{-1} = 5\ \mu\text{m}^{-1}$ (where strong absorption sets in) rather than at $\lambda^{-1} = 20$ for the bare 0.01-μm particles. If there are substantial numbers of still smaller bare particles they might still have sufficient temperature fluctuations to prevent accretion. However, it is clear that even if we start with grains which normally give very high UV extinction, when they go to form dark clouds they must lose the ability to produce the sharp rise in extinction labeled '4' in Figure 1. It is important to realize here that if the 'bare' particles are adding mantles they start contributing to the classical extinction range '2' as additional small core-mantle particles while at the same time the already existing core-mantles are growing. Further investigation of this process (Greenberg and Hong, 1974b) leads to the conclusion that the bare particles must be inhibited from accreting even in very dense clouds.

(d) H II REGIONS

The process of star formation starting with condensation in dark clouds leads to effects on the grains inverse to those in dark clouds. When the star is turned on, and

https://doi.org/10.1017/S0074180900026395 Published online by Cambridge University Press

even before, in the not too distant regions of the solar nebula, the grains are elevated in temperature so that the mantles must evaporate. If the star is very hot then in the H II region the sputtering mechanism also becomes operative and the strong ultraviolet extinction component should reappear as the particles lose their mantles. However, as already mentioned the classical extinction should not be grossly modified. In general, dust associated with young H II regions will have depleted but still larger than normal mantles and relatively weak ultraviolet extinction.

VIII. Concluding Remarks

Cosmic abundance considerations lead very strongly to a silicate core-ice mantle model for the grains. The depletion of the atoms heavier than O, C, N observed by Copernicus is another indication of this type of grain composition. The far-ultraviolet extinction curves imply an additional population of dust grains which is much smaller than those which are generally considered as cores for the accretion of condensible atoms. A temperature-fluctuation mechanism is proposed to account for the distinction in accretion capabilities of these very small particles. A specific preliminary core-mantle cylinder model seems to offer a basis for establishing the connection with observations of grain variability. Detailed calculations are in progress in order to make more definitive predictions of the dependence of extinction and polarization through the entire observed spectral ranges on local conditions and the past history of the grains.

Acknowledgement

This work was supported in part by NASA grant #NGR-33-011-043.

References

Bless, R. C. and Savage, B. C.: 1972, *Astrophys. J.* **171**, 293.
Borgman, J.: 1973, *Space Sci. Rev.* **15**, 121.
Cameron, A. G. W.: 1973, preprint.
Cayrel, R. and Schatzman, E.: 1954, *Ann. Astrophys.* **17**, 555.
Gilra, D. P.: 1971, *Nature* **229**, 237.
Gillett, F. C. and Forrest, W. J.: 1973, *Astrophys. J.* **179**, 483.
Greenberg, J. M.: 1960, *J. Appl. Phys.* **31**, 82.
Greenberg, J. M.: 1968, *Stars and Stellar Systems* **7**, Ch. 6.
Greenberg, J. M.: 1969, *Physica* **41**, 67.
Greenberg, J. M.: 1971, *Astron. Astrophys.* **12**, 240.
Greenberg, J. M.: 1973a, *On the Origin of the Solar System* (Proc. of Symposium, Nice, France, April 1972, Centre National de la Recherche Scientifique, 1973), p. 135.
Greenberg, J. M.: 1973b, in M. A. Gordon and L. E. Snyder (eds.), *Molecules in the Galactic Environment*, John Wiley and Sons, p. 93.
Greenberg, J. M.: 1973c, 'Interstellar Dust and Related Topics', *IAU Symp.* **52**, 3.
Greenberg, J. M. and Hong, S. S.: 1974a, in A. G. W. Cameron and G. B. Field (eds.), *Proc. of the 'Dusty Universe Symp.'*, Cambridge, Mass. 1973, in press.
Greenberg, J. M. and Hong, S. S.: 1974b, *Proc. of 8th ESLAB Symp. on* H II *Regions and Galatic Center*, Frascati, Italy, 1974, in press.
Greenberg, J. M., Lind, A. C., Wang, R. T., and Libelo, L. F.: 1963a, *Electromagnetic Scattering* (Proc. of

Interdisciplinary Conf. held at Clerkson College of Technology, Potsdam, New York, August 1962), p. 123.
Greenberg, J. M., Libelo, L. F., Lind, A. C., and Wang, R. T.: 1963b, in E. C. Jordan (ed.), *Electromagnetic Theory and Antennas*, Macmillan Co., New York, Part. 1, p. 81.
Greenberg, J. M., Yencha, A. J., Corbett, J. W., and Frisch, H. L.: 1972, *Mem. Soc. Roy. Sci. Liège*, 6e series, 3.
Greenstein, J. L.: 1938, *Harvard Obs. Circ.*, No. 442.
Hall, J. S.: 1949, *Science* **109**, 166.
Hiltner, W. A.: 1949, *Science* **109**, 165.
Hoyle, F. and Wickramasinghe, N. C.: 1962, *Monthly Notices Roy. Astron. Soc.* **124**, 417.
Huffman, D. R. and Stapp, J. L.: 1971, *Nature Phys. Sci.* **229**, 45.
Hulst, H. C. van de: 1943, *Ned. Tijdschr. v. Natuurkunde* **10**, 251.
Hulst, H. C. van de: 1946, *Rech. Astron. Obs. Utrecht*, ii, Part 1.
Hulst, H. C. van de: 1957, *Light Scattering by Small Particles*, John Wiley and Sons, Inc., New York; Chapman and Hall, Ltd., London.
Kamijo, F.: 1963, *Publ. Astron. Soc. Japan* **15**, 440.
Kamijo, F. and Jong, T. de: 1973, *Astron. Astrophys.* **25**, 371.
Kemp, J. C.: 1973, in J. M. Greenberg and H. C. van de Hulst (eds.), 'Interstellar Dust and Related Topics', *IAU Symp.* **52**, 181.
Kittel, C.: 1956, *Solid State Physics*, John Wiley and Sons, Inc., New York, p. 130.
Lind, A. C. and Greenberg, J. M.: 1966, *J. Appl. Phys.* **37**, 3195.
Lindblad, B.: 1935, *Nature* **135**, 133.
Lynds, B. T.: 1970, in K. O. Kiepenheuer (ed.), 'The Spiral Structure of Our Galaxy', *IAU Symp.* **38**, 26.
Martin, P. G.: 1973, in J. M. Greenberg and H. C. van de Hulst (eds.), 'Interstellar Dust and Related Topics', *IAU Symp.* **52**, 161.
Martin, P. G., Illing, K., and Angel, J. R. P.: 1973, 'Interstellar Dust and Related Topics', *IAU Symp.* **52**, 169.
Morton, D. C., Drake, J. F., Jenkins, E. B., Rogerson, J. B., Spitzer, L., and York, D. G.: 1973, *Astrophys. J.* **181**, L103.
Oort, J. H. and Hulst, H. C. van de: 1946, *Bull. Astron. Inst. Neth.* **10**, 187.
Platt, J. R.: 1956, *Astrophys. J.* **193**, 486.
Rogerson, J. B., York, D. G., Drake, J. F., Jenkins, E. B., Morton, D. C., and Spitzer, L.: 1973, *Astrophys. J.* **181**, L110.
Schalén, C.: 1936, *Medd. Uppsala Astron. Obs.* **64**.
Shah, G. A.: 1970, *Monthly Notices Roy. Astron. Soc.* **148**, 93.
Whiteoak, J. B.: 1966, *Astrophys. J.* **144**, 305.
Woolf, N. J.: 1973, in J. M. Greenberg and H. C. van de Hulst (eds.), 'Interstellar Dust and Related Topics', *IAU Symp.* **52**, 485.
York, D. G., Drake, J. F., Jenkins, E. B., Morton, D. C., Rogerson, J. B., and Spitzer, L.: 1973, *Astrophys. J.* **182**, L1.

J. Mayo Greenberg
Seung-Soo Hong
State University of New York at Albany,
Astronomy and Space Science Department,
Albany, N.Y. 12222, U.S.A.

DISCUSSION

Wynn-Williams: The OAO data indicate a correlation between the slope of the extinction curve at about 1000 Å and the prominence of the 2200 Å peak. Does your model take any account of this?

Greenberg: Qualitatively the answer must be yes although we have not carried out any detailed calculations on this. Within the framework of our bi-modal model consisting of relatively large core-mantle particles and very small bare particles, it is the bare particles which would produce both the bump and the far UV extinction. Under those conditions in which the core mantle particles have larger than normal mantles the far UV extinction is obviously reduced along with the relative size of the 2200 Å bump.